Biochemistry and Biophysics Reports 5 (2016) 272–284

Contents lists available at ScienceDirect

Biochemistry and Biophysics Reports

journal homepage: www.elsevier.com/locate/bbrep

A new lysine derived glyoxal inhibitor of trypsin, its properties and utilization for studying the stabilization of tetrahedral adducts by trypsin

Jennifer A. Cleary, J. Paul G. Malthouse *

School of Biomolecular and Biomedical Science, Centre for Synthesis and Chemical Biology, Conway Institute, University College Dublin, Dublin 4, Ireland

ARTICLE INFO

Article history:
Received 10 November 2015
Received in revised form
22 December 2015
Accepted 30 December 2015
Available online 4 January 2016

Keywords:
NMR
Trypsin
Serine protease
Glyoxal inhibitor
Tetrahedral intermediate
Schiff Base: lysine

ABSTRACT

New trypsin inhibitors Z-Lys-COCHO and Z-Lys-H have been synthesised. K_i values for Z-Lys-COCHO, Z-Lys-COOH, Z-Lys-H and Z-Arg-COOH have been determined. The glyoxal group (–COCHO) of Z-Lys-COCHO increases binding ~300 fold compared to Z-Lys-H. The α-carboxylate of Z-Lys-COOH has no significant effect on inhibitor binding. Z-Arg-COOH is shown to bind ~2 times more tightly than Z-Lys-COOH. Both Z-Lys-^{13}COCHO and Z-Lys-CO^{13}CHO have been synthesized. Using Z-Lys-^{13}COCHO we have observed a signal at 107.4 ppm by ^{13}C NMR which is assigned to a terahedral adduct formed between the hydroxyl group of the catalytic serine residue and the ^{13}C-enriched keto-carbon of the inhibitor glyoxal group. Z-Lys-CO^{13}CHO has been used to show that in this tetrahedral adduct the glyoxal aldehyde carbon is not hydrated and has a chemical shift of 205.3 ppm. Hemiketal stabilization is similar for trypsin, chymotrypsin and subtilisin Carlsberg. For trypsin hemiketal formation is optimal at pH 7.2 but decreases at pHs 5.0 and 10.3. The effective molarity of the active site serine hydroxyl group of trypsin is shown to be 25300 M. At pH 10.3 the free glyoxal inhibitor rapidly ($t_{1/2}$=0.15 h) forms a Schiff base while at pH 7 Schiff base formation is much slower ($t_{1/2}$=23 h). Subsequently a free enol species is formed which breaks down to form an alcohol product. These reactions are prevented in the presence of trypsin and when the inhibitor is bound to trypsin it undergoes an internal Cannizzaro reaction via a C2 to C1 alkyl shift producing an α-hydroxycarboxylic acid.

1. Introduction

With peptide substrates catalysis by the serine proteases proceeds via a tetrahedral intermediate formed by the addition of the catalytic serine hydroxyl group to the peptide carbonyl carbon [1,2]. It is the formation or breakdown of this tetrahedral intermediate that is the rate limiting step in catalysis with peptide substrates. Therefore it is important to determine how transition state stabilization of the tetrahedral intermediate contributes to catalysis. Such tetrahedral intermediates do not accumulate during the enzyme catalysed hydrolysis of peptide bonds [3] and so they cannot be studied directly by techniques such as NMR. However, inhibitors which react with the hydroxyl group of the catalytic serine to form transition state analogues [4] of the tetrahedral intermediate can be used to determine how the serine proteases form and stabilize tetrahedral intermediates. Extensive ^{13}C NMR studies have been undertaken on tetrahedral adducts formed by chloromethylketone derivates of subtilisin [5–8], chymotrypsin [6,8–10] and trypsin [11–13]. However, these chloromethylketone inhibitors are irreversible inhibitors that alkylate the catalytic histidine moving the catalytic groups out of their optimal positions [14]. Therefore they may not be good mimics of the catalytic tetrahedral intermediate. Also as they are irreversible inhibitors we cannot use them to quantify inhibitor binding.

Specific peptide derived glyoxal inhibitors are formed by replacing the carboxy-terminal carboxylate group (R–COOH) of a peptide with a glyoxal group (R–COCHO). These glyoxal inhibitors have been shown to be potent reversible competitive inhibitors of chymotrypsin [15–18] and subtilisin [19,20]. Using ^{13}C NMR these glyoxal inhibitors have been shown to form tetrahedral adducts with both chymotrypsin [15,17,21] and subtilisin [19,20] which have been characterized by NMR. We have also developed a procedure whereby we replace the terminal carboxylate group (R–COOH) of a peptide with a hydrogen atom (R–H). If we assume this hydrogen atom does not make a significant contribution to binding then the binding of R–H will allow us to determine how much the peptide component contributes to binding. If we also measure the binding of an equivalent peptide carboxylate (R–COOH), aldehyde (R–CHO) or glyoxal (R–COCHO) inhibitor then we can

Abbreviations: Z, benzyloxycarbonyl; Z-Lys-H, Z-NHCH$_2$(CH$_2$)$_4$NH$_3^+$; Z-Lys-COOH, Z-NHCH((CH$_2$)$_4$NH$_3^+$)-COOH; Z-Lys-COCHO, Z-NHCH((CH$_2$)$_4$NH$_3^+$)-COCHO

* Correspondence to: School of Biomolecular and Biomedical Science, Centre for Synthesis and Chemical Biology, Conway Institute, University College Dublin, Dublin 4, Ireland.

E-mail address: J.Paul.G.Malthouse@ucd.ie (J.P.G. Malthouse).

http://dx.doi.org/10.1016/j.bbrep.2015.12.015

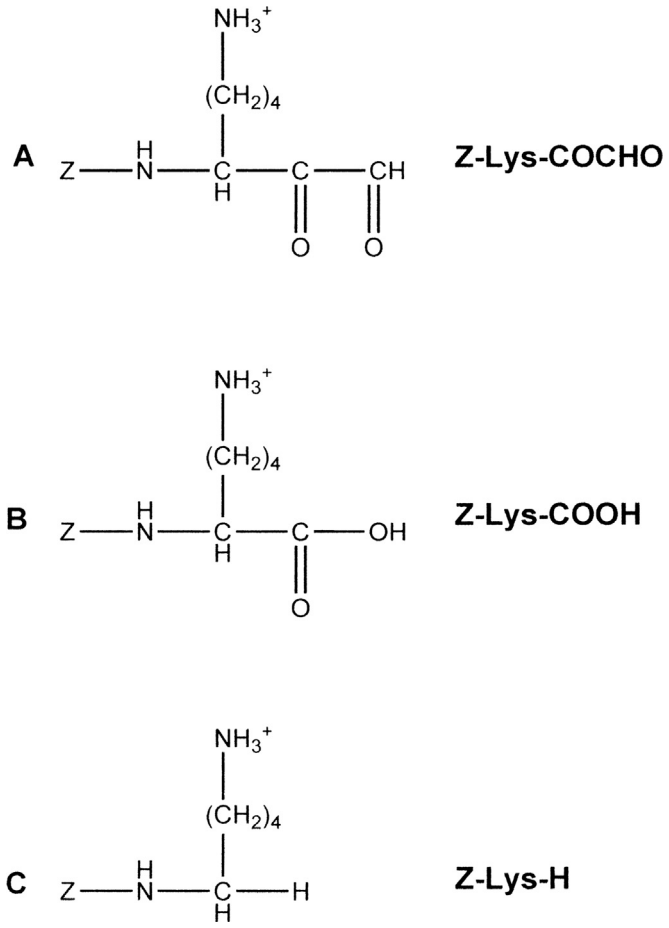

Scheme 1. Structure of Inhibitors.

quantify how the carboxylate, aldehyde and glyoxal group contribute to binding by the enzyme [22–24]. This approach has allowed us to quantify hemiketal formation in both chymotrypsin and subtilisin. The effective molarity of the catalytic serine hydroxyl group is the concentration of water required to have the same reactivity as the catalytic hydroxyl group of the serine protease. Therefore the effective molarity quantifies how the serine proteases enhance the reactivity of the catalytic serine hydroxyl group. This approach has been used to determine the effective molarity of the catalytic serine hydroxl group in both chymotrypsin and subtilisin [24]. A similar approach has been used to determine the effective molarity of the catalytic thiol group of the cysteine protease papain [23]. However, similar studies have not been carried out using specific positively charged glyoxal inhibitors of the serine protease trypsin. The synthesis of positively charged glyoxal inhibitors such as Z-Lys-glyoxal is difficult because the reactive ε-amino group must be protected during the synthesis.

In this paper we report the first synthesis of a glyoxal inhibitor (Z-Lys-COCHO) of trypsin. Z-Lys-H and the ^{13}C-enriched glyoxal inhibitors Z-Lys-^{13}COCHO and Z-Lys-CO^{13}CHO have also been synthesized. The ^{13}C-enriched inhibitors have enabled us to use ^{13}C NMR to study the stability of the inhibitor and to determine its breakdown products. We have quantified hemiketal formation with trypsin and Z-Lys-COCHO at pH 7.2 and compared it with hemiketal formation by chymotrypsin and subtilisin. This has allowed us to determine the effective molarity of the catalytic serine hydroxyl in trypsin and compare it with the effective molarity of the catalytic serine hydroxyl group in subtilisin and chymotrypsin. ^{13}C NMR with both ^{13}C-enriched glyoxal inhibitors is used to determine the structure of the Z-Lys-COCHO inhibitor when it is bound to trypsin. Finally it is shown that the enzyme catalysed breakdown of the Z-Lys-COCHO is different from its breakdown in the absence of trypsin.

2. Materials and methods

2.1. Materials

Z-Lys(Boc) was obtained from Fluorochem Ltd, Unit 14, Graphite Way, Hadfield, Derbyshire, SK13 1QH, UK. L-[1-^{13}C]lysine:2HCl (99 at%) and [^{13}C]methylamine:HCl (99 at%) were obtained from Goss Scientific Instruments Ltd, Gresty Lane, Shavington, Crewe, Cheshire, CW2 5DD, UK. All other reagents were obtained from Sigma-Aldrich Chemical Co., Gillingham, Dorset, U.K.

2.2. Synthesis of Z-Lys-COCHO

Z-Lys(Boc) was converted to Z-Lys(Boc)-diazoketone as described by Cosgrove et al. [25] After purification by silica column chromatography the Z-Lys(Boc)-diazoketone was oxidised to Z-Lys (Boc)-glyoxal using dimethyldioxirane as described by Howe et al. [26] The t-butoxycarbonyl group(Boc) was removed by treating Z-Lys(Boc)-glyoxal in methanol with an equal volume of 1.25 M methanolic HCl for two hours at room temperature. The methanol was removed in vacuo, the product was dissolved in water and the pH adjusted to 3.0, filtered under suction and freeze-dried. The dried product was dissolved in d_6 DMSO.

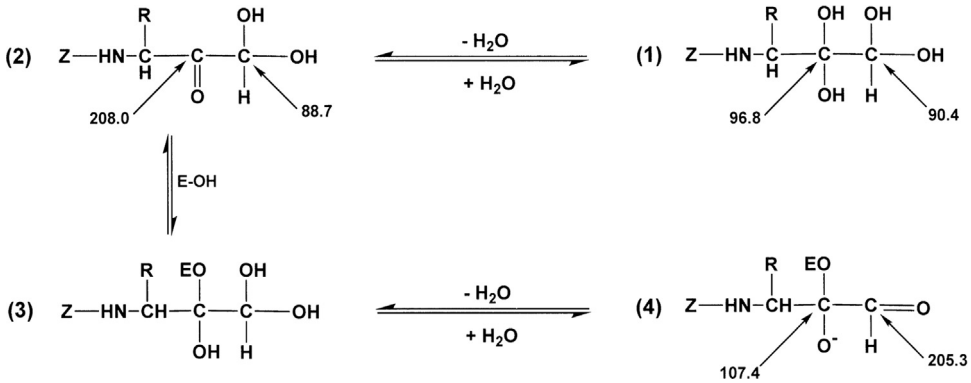

Scheme 2. Reaction of Z-lys-COCHO with trypsin R=–$(CH_2)_4$–NH_3^+, EO represents the oxygen atom of the catalytic serine hydroxyl group of trypsin.

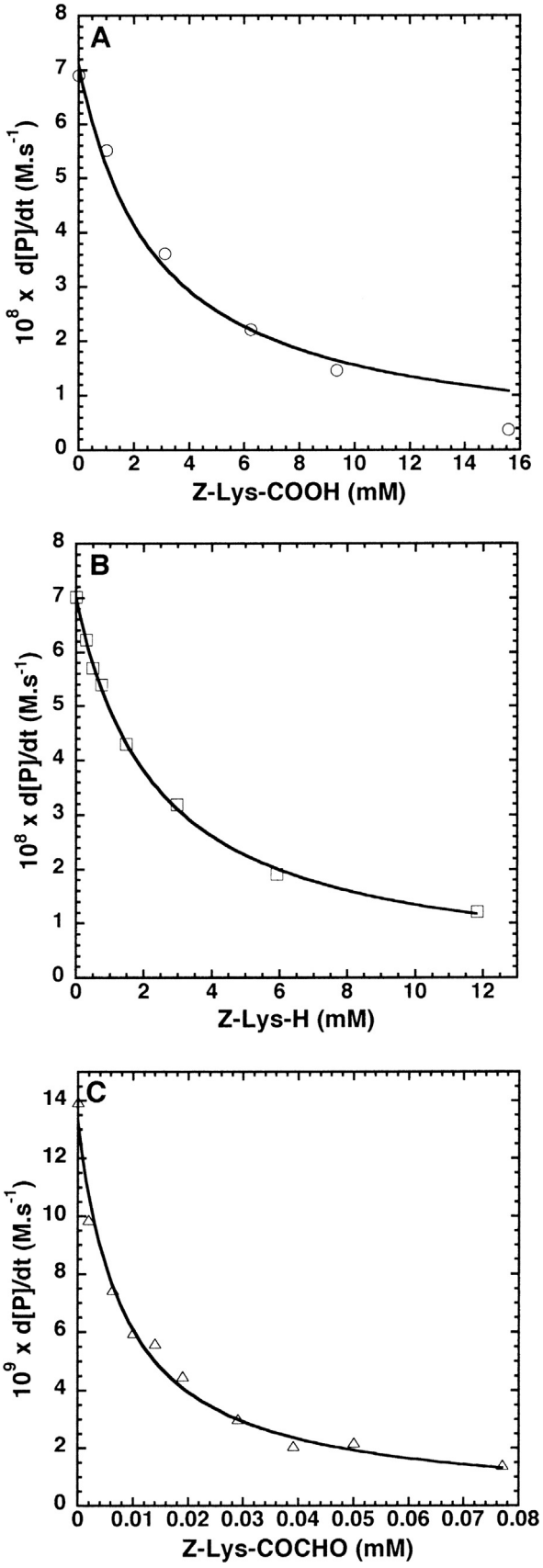

Fig. 1. Inhibition of the trypsin catalysed hydrolysis of α-N-benzoyl-L-arginine-p-nitroanilide by Z-Lys-COOH, Z-Lys-H and Z-Lys-COCHO at pH 7.2 and 25 °C. All samples contained 3.3% (v/v) dimethyl sulphoxide and 0.1 M potassium phosphate buffer. The solid lines were calculated using the equation $d[P]/dt = v_o \cdot K_i/([I]+K_i)$ and the fitted values of v_o ($v_o = (k_{cat}/K_M)[E_o][S_o]$) and K_i. Fitted values for v_o and K_i were respectively: (a) Z-Lys-COOH; $7.09 \pm 0.39 \times 10^{-8}$ M s^{-1} and 2.81 ± 0.49 mM, (b) Z-Lys-H; $7.00 \pm 0.05 \times 10^{-8}$ M s^{-1} and 2.38 ± 0.07 mM, (c) Z-Lys-COCHO; $7.85 \pm 0.18 \times 10^{-9}$ M s^{-1} and 8.44 ± 0.80 μM. For inhibition by Z-Lys-COOH and Z-Lys-H substrate and trypsin concentrations were 91.3 μM and 0.95 μM respectively. For inhibition by Z-Lys-COCHO substrate and trypsin concentrations were 88.0 μM and 0.17 μM respectively.

Table 1
Binding of inhibitors to trypsin.

Enzyme	pH	$K_{i(obs)}$ (μM)[a]			K_{iH}/K_{iCOOH}	K_{iH}/K_{iCOCHO}
		ZK-H	ZK-COOH	ZK-COCHO	$K_{iZK-H}/K_{iZKCOOH}$	$K_{iZK-H}/K_{iZKCOCHO}$
Trypsin	7.2	2240 ± 290	2790 ± 30	8.20 ± 0.53	0.80	273
			ZR-COOH			
Trypsin	7.2		1230 ± 30			

[a] Errors are the standard deviations of 3 or more determinations.

2.3. NMR Spectrum of Z-Lys-COCHO

Due to residual water in the d_6-DMSO solvent the aldehyde group of Z-Lys-COCHO was hydrated (Z-Lys-COCH$(OH)_2$). ^{13}C NMR analysis of Z-Lys-COCH$(OH)_2$ gave the following data (75.468 MHz, d_6-DMSO) δ: 22.67 (1C, $NH_2CH_2CH_2\underline{C}H_2CH_2$), 26.56 (1C, $NH_2CH_2\underline{C}H_2CH_2CH_2$), 29.19 (1C, $NH_2CH_2CH_2CH_2\underline{C}H_2$), ~40.00[1] (1C, $NH_2\underline{C}H_2CH_2CH_2CH_2$), 55.87 (1C, $CH_2\underline{C}HC{=}OCH(OH)_2$), 65.57 (1C, O-$\underline{C}H_2$Ph), 89.12, (1C, $CHC{=}O\underline{C}H(OH)_2$), 127.50-128.5 (5C, $\underline{C}H{=}CH$), 137.08 (1C, $CH{=}\underline{C}{=}$), 156.22 (1C, $NH\underline{C}{=}O$), 206.81 (1C, $CH\underline{C}{=}OCH(OH)_2$).

2.4. Synthesis of Z-Lys-^{13}COCHO and Z-Lys-CO^{13}CHO

These were synthesized as described for the un-enriched compound (See Section 2.2) except that [^{13}C]methylamine was used to synthesize the diazomethane used to produce Z-Lys-CO^{13}CHO and L-[1-^{13}C]lysine was used to synthesize Z-Lys-^{13}COCHO. L-[1-^{13}C]lysine was converted to Z-Lys(Boc)-^{13}COOH as described by Wiejak et al. [27].

2.5. NMR SPECTRA OF z-Lys-^{13}Cocho AND z-Lys-CO^{13}CHO

In 1 mM HCl Z-Lys-^{13}COCHO (Scheme 1A) gave two large signals one at 208.0 (Structure 2 in Scheme 2) and the other at 96.8 ppm (Structure 1 in Scheme 2) due to the ^{13}C-enriched glyoxal keto carbon and its hydrate respectively. For Z-Lys-CO^{13}CHO in 1 mM HCl there were also two large signals due to the ^{13}C-enriched hydrated glyoxal aldehyde carbonyl carbon at 90.4 and 88.7 ppm. The signal at 88.7 ppm is due to the hydrated glyoxal aldehyde carbon when the glyoxal keto carbon is not hydrated (Structure 2 in Scheme 2) and the signal at 90.4 ppm is due to the hydrated glyoxal aldehyde carbon when the glyoxal keto carbon is hydrated (Structure 1 in Scheme 2).

2.6. Trypsin

Trypsin was obtained from Sigma as a crystallized and lyophilized powder. The trypsin was 78% fully active by active site titration with p-nitrophenyl p-guanidobenzoate [28] as described by Malthouse et al. [12]

2.7. Determination of K_i values

The inhibition of the trypsin catalysed hydrolysis of α-N-benzoyl-L-arginine-p-nitroanilide was studied at 25 °C in 3 ml cuvettes and 0.1 M buffers as described previously for the α-

[1] This signal was obscured by the signal from d_6-DMSO, its chemical shift is estimated from its chemical shift of 40.60 ppm in 90% (v/v) H_2O and 10% (v/v) ^2H_2O.

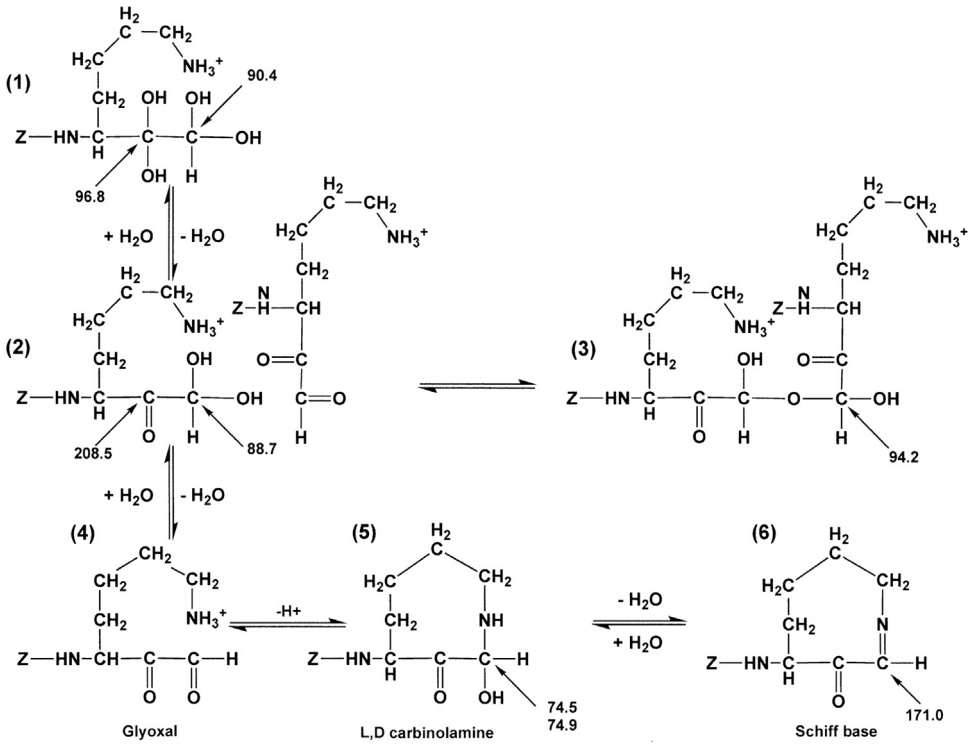

Scheme 3. Reactions of Z-Lys-COCHO at pH 3 after 1 year.

chymotrypsin catalysed hydrolysis of suc-Phe-pNA at pHs 7.2 and 10.6 [24] except at pH 5.0 where a 0.1 M sodium acetate buffer was used. K_i values were determined when $[S_o] \ll [K_M]$ as previously described [24]. Initial rates were completed within 0.5 to 1 min to ensure there was not a significant loss of inhibitor by Schiff base formation (see Section 3.3 for further details).

2.8. NMR spectroscopy

NMR spectra at 11.75 T were recorded with a Bruker Avance DRX 500 standard-bore spectrometer operating at 125.7716 MHz for ^{13}C-nuclei. 10 mm-diameter NMR tubes containing ~3 mL samples were used for ^{13}C NMR spectroscopy. Waltz- 16 composite pulse ^{1}H decoupling of 1.0 W was used which was reduced to 0.026 W during the relaxation delay to minimize dielectric heating but maintain the Nuclear Overhauser Effect. All other ^{13}C NMR spectral conditions are described in the appropriate figure legends. All samples were at 25 °C and contained 10% (v/v) $^{2}H_2O$ which was used as a deuterium lock signal.

The ^{13}C chemical shifts are quoted relative to tetramethylsilane at 0.00 p.p.m. The chemical shift of d_6-dimethyl sulphoxide (< 5% (v/v)) at 38.7 ppm was used as a secondary reference for ^{13}C NMR spectra obtained in aqueous solutions.

3. Results

3.1. Binding of Z-Lys-H, Z-Lys-COOH and Z-Arg-COOH to trypsin.

Binding was determined by studying the inhibition of the trypsin catalysed hydrolysis of α-N-benzoyl-L-arginine-*p*-nitroanilide at pH 7.2 when $[S_o] \ll K_M$ (Fig. 1). Replacing the α-carboxyl group of Z-Lys-COOH (Scheme 1B) with a hydrogen atom to form Z-Lys-H (Scheme 1C) did not have a significant effect on binding (Table 1). This is in contrast to the results obtained with α-chymotrypsin and subtilisin Carlsberg where there was 3–4 fold tighter binding when the α-carboxylate groups of Z-Ala-Ala-Phe-COOH and Z-Ala-Pro-Phe-COOH were replaced by a hydrogen atom [24]. Z-Arg-COOH was bound ~2 × more tightly by trypsin than Z-Lys-COOH (Table 1).

3.2. ^{13}C NMR spectra of Z-Lys-CO^{13}CHO at pH 3.0

At pH 3.0 two large signals were observed one due to the hydrated aldehyde carbon of the inhibitor at 90.4 ppm when the glyoxal keto carbon was also hydrated (Structure 1 in Scheme 2) and one at 88.7 ppm when the glyoxal keto carbon was not hydrated (Structure 2 in Scheme 2). The signals at 88.7 and 90.4 ppm had T_1 values of 1.6 ± 0.1 s and 0.79 ± 0.03 s respectively at pH 3.0. No new ^{13}C NMR signals were detected and no change in the intensity of the NMR signals were observed after 64 h at 25 °C. However, after storage for ~1 year at pH 3 the signals at 90.4 and 88.7 ppm decreased in intensity ($t_{1/2}$ = 77.1 ± 9.5 days) and new signals at 94.2 (J_{CH} = 175.2 ± 0.2), 74.9 (J_{CH} = 163.1 ± 0.2) and 74.5 (J_{CH} = 161.5 ± 0.2) ppm were observed. The signal at 94.2 ppm is assigned to intermolecular hemiacetal formation (Structure 3 in Scheme 3) and the signals at 74.9 and 74.5 ppm are assigned to the formation of two diastereomeric carbinolamines (Structure 5 in Scheme 3) formed by intramolecular cyclisation of the glyoxal inhibitor (Structure 4 and 5 in Scheme 3). Similar diastereomeric intramolecular carbinolamines have been formed between the argino group and the aldehyde group of the aldehyde inhibitor leupeptin [29]. On adjusting the pH to 7.2 or 10.2 all these signals were replaced by a single signal at 171.0 ppm (Structure 6 in Scheme 3) due to Schiff base formation (see next section for details).

3.3. ^{13}C NMR of Schiff base formation by Z-Lys-CO^{13}CHO

At pH 7.2 there was a 1st order decrease in the intensity of the signals at 88.7 and 90.4 ppm due to the hydrated ^{13}C-enriched

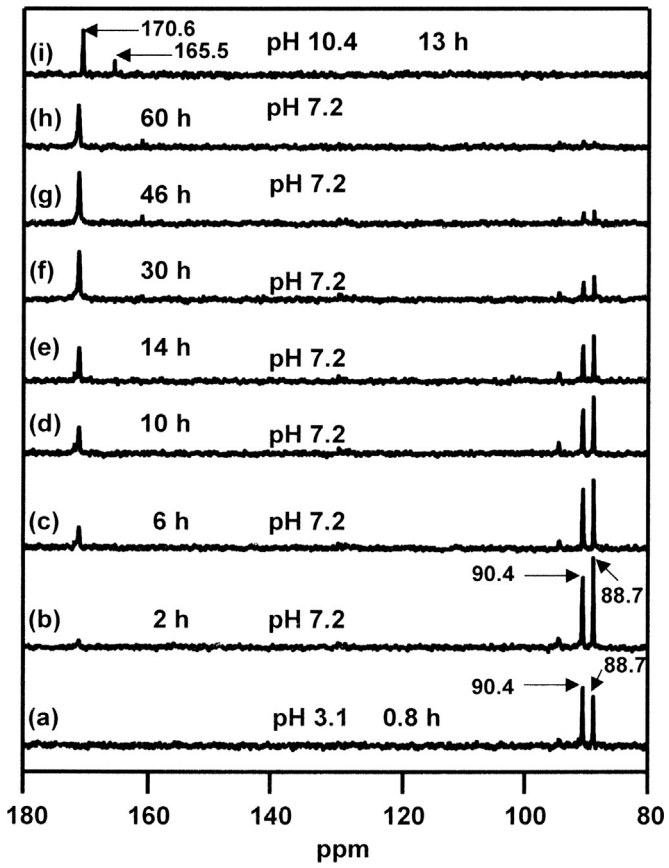

Fig. 2. ^{13}C NMR of Schiff base formation by Z-Ls-CO^{13}CHO at pH 7.2. The conditions used for proton decoupling are described in the Materials and methods section, NMR parameters were: 16384 time domain points; spectral width 219.2 ppm; acquisition time 0.59 s; 1.5 s relaxation delay time; 90° pulse angle; exponential weighting factor of 10 Hz. The number of transients recorded per spectrum were 6656 for spectra (b)–(h) and 512 for spectra (a) and (i). Sample conditions were: (a) 2.75 ml of 1.2 mM Z-Lys-CO^{13}CHO, ~1 mM HCl, pH 3.1; (b)–(h) 3 ml of 1.1 mM Z-Lys-CO^{13}CHO, 20 mM potassium phosphate buffer, pH 7.2; (i) 3 ml of 1.1 mM Z-Lys-CO^{13}CHO, 20 mM sodium bicarbonate buffer, pH 10.4.

glyoxal aldehyde carbon of Z-Lys-CO^{13}CHO and a concomitant 1st order increase in the intensity of a new signal at 170.6 ppm (Fig. 2a–h). The 1st order rate constant for this reaction was $0.062 \pm 0.016\ h^{-1}$ corresponding to a half life of 11.2 h for this reaction. When determining K_i values for the inhibition of trypsin by Z-Lys-COCHO at pH 7.2, the inhibitor was added last and the initial rates were completed within 1 min. In that time no more than 0.1% of the inhibitor will be converted to the Schiff base. Therefore we can neglect this reaction when determining the binding parameters of Z-Lys-COCHO to trypsin at pH 7.2 (Scheme 4). The chemical shift of the new signal titrated from 177.34 ± 0.037 to 170.54 ± 0.036 ppm as the pH increased with a pKa of 6.24 ± 0.03 (Fig. 3A). These chemical shift values are typical of protonated and neutral aliphatic aldimines/ Schiff bases [30,31] and also of protonated and ionised carboxylic acids [32]. However, in contrast the chemical shift of a carboxylic acid increases as it ionises and they usually have pKa values of 2–4. Schiff bases/imines typically have pKa values of ~7 [33] which is close to the observed pKa. In the absence of proton decoupling a doublet was formed confirming that there was one directly bonded proton. The coupling constant J_{CH} decreased from 183.06 ± 0.09 Hz to 175.42 ± 0.08 Hz with a pKa of 6.18 ± 0.07 (Fig. 3B). With the exception of formic acid (pKa=3.74), carboxylic acids do not have directly bonded protons and so this confirms that the signal is not due to a carboxylic acid and that a Schiff base has been formed (Structure 6 in Scheme 3) with a pKa ~6.2 (Structures 2–3 in Scheme 5) by dehydration of the carbinolamine (Structure 5 in Scheme 3). At pH 10.4 there was rapid formation of a signal at 170.6 ppm (Fig. 2i) due to the formation of a Schiff base. This reaction was quicker than at pH 7.2 with a 1st order rate constant of $4.7 \pm 0.7\ h^{-1}$ corresponding to a half life of 0.15 h. The signal at 165.5 ppm (Fig. 2i) is due to the 20 mM sodium bicarbonate buffer used to maintain the pH.

At pH 10.3, 7.5% of the inhibitor would form an aldimine/ Schiff base in the 1st minute of the reaction while after 5 min 32% of Z-Lys-COCHO would form an aldimine. Therefore all initial rates used to determine the K_i values of Z-Lys-COCHO at pH 10.3 were obtained within 0.5–1 min of adding the inhibitor to a solution of enzyme and substrate ensuring that < 7.5% of the inhibitor was lost during the initial rate measurement.

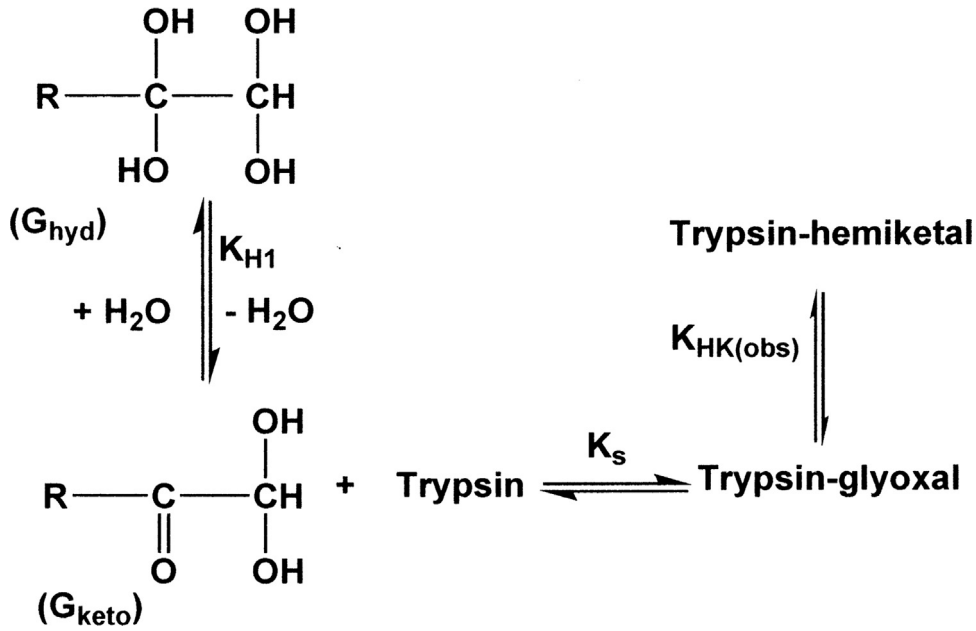

Scheme 4. Minimal scheme for hemiketal formation between Trypsin and Z-Lys-COCHO.

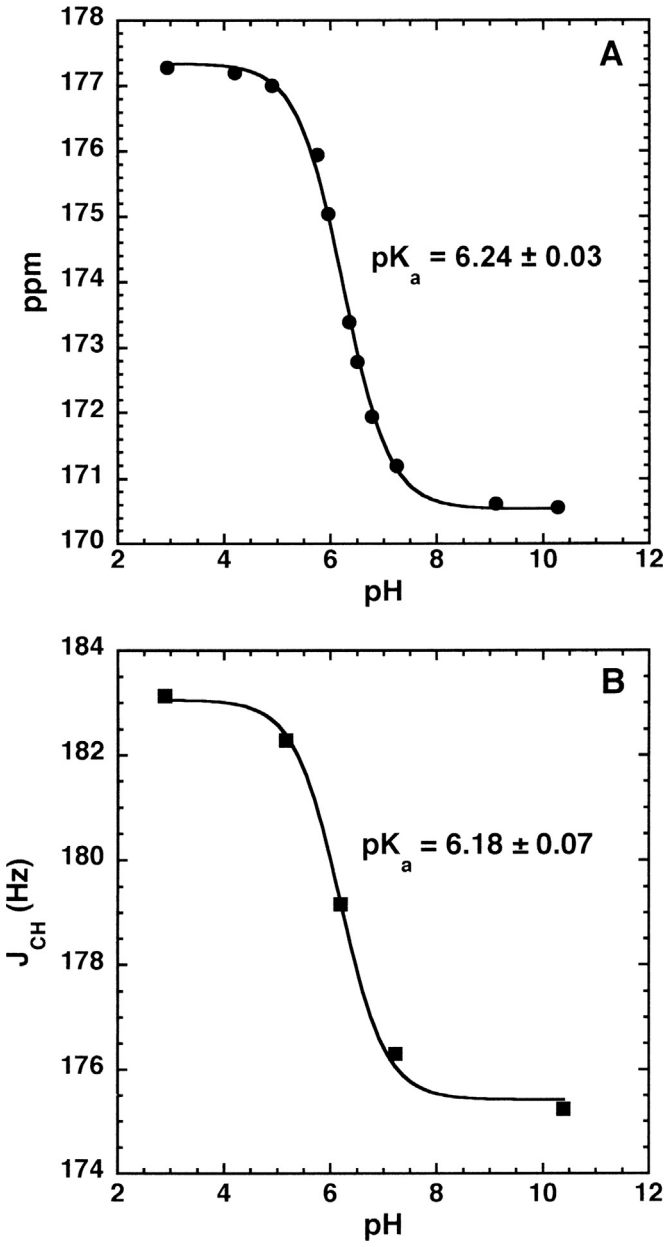

Fig. 3. Effect of pH on the chemical shifts and J_{CH} values of the ^{13}C NMR signals from the Schiff base formed from Z-Lys-CO^{13}CHO. In (A) the continuous line was calculated using the equation $\delta_{obs}=\delta_1/(1+K_a/[H])+\delta_2/(1+[H]/K_a)$ and the fitted parameters pKa = 6.24 ± 0.03, δ_1 = 177.34 ± 0.037 ppm and δ_2 = 170.54 ± 0.036 ppm. In (B) the continuous line was calculated using the equation $J_{CH}=J_1/(1+K_a/[H])+J_2/(1+[H]/K_a)$ and the fitted parameters pKa = 6.18 ± 0.07, J_1 = 183.06 ± 0.09 Hz and J_2 = 175.42 ± 0.08 Hz.

3.4. ^{13}C NMR of Schiff base formation by Z-Lys-^{13}COCHO at neutral and alkaline pH values

At pH 3.4 signals at 208.0 and 96.8 ppm due to the ^{13}C-enriched keto carbon of Z-Lys-^{13}COCH(OH)$_2$ (Structure 2 in Scheme 2) and its hydrate Z-Lys-^{13}C(OH)$_2$CH(OH)$_2$ (Structure 1 in Scheme 2) had T_1 values of 7.0 ± 0.5 s^{-1} and 7.4 ± 0.3 s^{-1} respectively. At pH 7.0 the intensity of the signals at 208.0 and 96.8 ppm decreased with time and there was a concomitant increase in the intensity of a new signal at 138.2 ppm (Fig. 4) with the low value of the coupling constant (J_{CCH} = 31.4 ± 0.2 Hz) confirming that the carbon with a signal at 138.2 ppm (Structures 2 and 3 in Scheme 5) does not have a directly bonded proton. The 1st order rate constant for this reaction was 0.030 ± 0.004 h^{-1} corresponding to a half life of 23.0 h. If we allow for the fact that this reaction was carried out at pH 7.0 and not 7.2 then the half life (14.5 h) for the formation of the signal at 138.2 ppm is very similar to that observed for the formation of the signal at 170.6 ppm ($t_{1/2}$ = 11.2 h) with Z-Lys-CO^{13}CHO (Fig. 2) which is expected as both should reflect the formation of the Schiff base. Intra-molecular dehydration should produce the Schiff base (Structure 1 in Scheme 5). The keto carbon in structure 1 in Scheme 5 is expected to have a chemical shift of ~200 pm while the observed chemical shift of 138.2 ppm shows that enolisation has occurred at this keto carbon [34] so that structures 2 and 3 in Scheme 5 initially predominate. However, the signal at 138.2 ppm decreased with time ($t_{1/2}$ ~ 70 h) and was replaced by a new signal at 76.5 ppm (Fig. 4). The signal at 161.1 ppm is due to bicarbonate. A coupled spectrum of the signal at 76.5 ppm revealed that it was a triplet (J_{CH} = 156.8 Hz) showing that the enol (structures 2 and 3 in Scheme 5) has been hydrolysed to give structures 4 and 5 in Scheme 5. The signals at 138.2 and 76.5 ppm titrated with pKa values of 6.16 ± 0.05 (Fig. 5A) and 6.28 ± 0.01 (Fig. 5B) respectively. These pKa values, as we saw with the Z-Lys-CO^{13}CHO, reflect ionization of the Schiff base carbon in the enolate (Structures 2 and 3 in Scheme 5) and alcohol forms (Structures 4 and 5 in Scheme 5). The structure of the Schiff base was maintained on forming the structures 1–5 in Scheme 5 and so it is not surprising that there was no significant perturbation of its chemical shift of 138.2 ppm over the time period when the signals at 138.2 and 76.5 ppm were observed.

3.5. Hydration of Z-Lys-CO^{13}CHO and Z-Lys-^{13}COCHO

^{13}C NMR of Z-Lys-^{13}COCHO at pH 3.0 revealed signals at 208.0 and 96.8 ppm due to the glyoxal keto carbon and its hydrate respectively (Fig. 6a). Using quantitative ^{13}C NMR it was estimated that for the glyoxal keto carbon K_{H1obs} = [hydrate]/[keto group] = 1.5 ± 0.1. ^{13}C NMR of Z-Lys-CO^{13}CHO at pH 3.0 showed that the glyoxal aldehyde group was hydrated with signals at 88.7 and 90.4 ppm being observed (Fig. 7a) due to the glyoxal keto carbon being dehydrated (RCOCH(OH)$_2$) or hydrated (RC(OH)$_2$CH(OH)$_2$ respectively [15]. There was also a small signal at 200.9 ppm (not shown in Fig. 7) due to the dehydrated aldehyde group which enabled us to determine that for the glyoxal aldehyde carbon of Z-Lys-CO^{13}CHO K_{H1obs} = 97 ± 7. Similar hydration constants have been determined in the same way for Z-Ala-Pro-Phe-COCHO [21] and Z-Ala-Ala-Phe-COCHO [24].

3.6. Binding of Z-Lys-COCHO to trypsin at pH 7.2.

The binding of Z-Lys-COCHO to trypsin was ~300 times better than that of Z-Lys-H to trypsin at pH 7.2 (Table 1). Similar results (450-2300) were obtained with tripeptide derived glyoxal inhibitors and chymotrypsin and subtilisin [24]. Therefore we can conclude that with both the trypsin and chymotrypsin serine proteases the glyoxal group can increase inhibitor binding by ~2 to 3 orders of magnitude.

3.7. Hemiketal formation with trypsin and Z-Lys-COCHO

The minimal scheme for hemiketal formation with trypsin and Z-lys-COCHO is expected to follow the same pathway (Scheme 4) described for chymotrypsin and subtilisin [24] with equations (1) and (2) defining the observed K_i ($K_{i(obs)}$) and the observed equilibrium constant ($K_{HK(obs)}$) for hemiketal formation respectively.

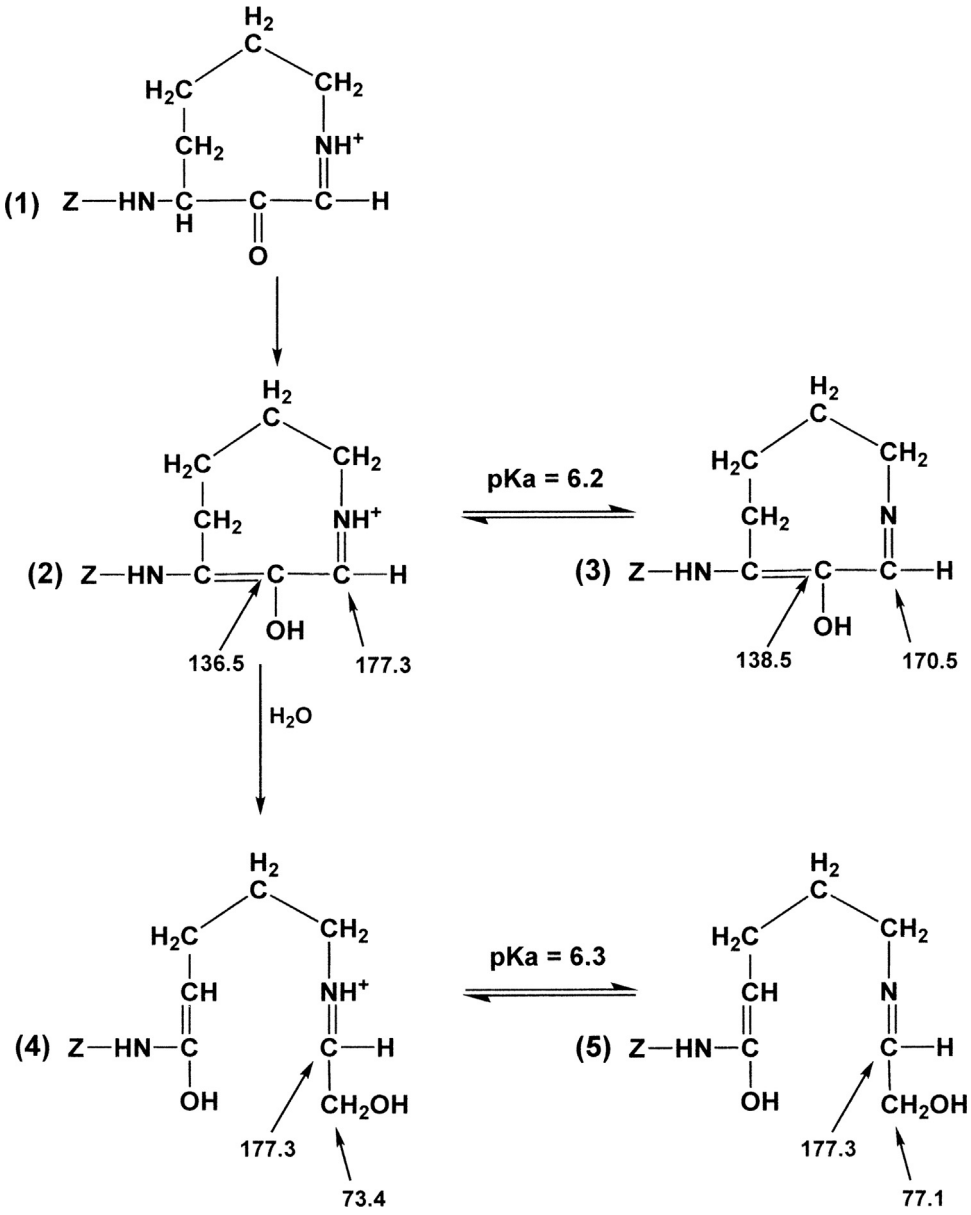

Scheme 5. Schiff bases formed from Z-Lys-COCHO.

$$K_{i(obs)} = K_s[1 + K_{H1(obs)}]/[1 + K_{HK(obs)}] \quad (1)$$

$$K_{HK(obs)} = \{K_s[1 + K_{H1(obs)}] - K_{i(obs)}\}/K_{i(obs)} \quad (2)$$

The hydration constant ($K_{H1} = [G_{hyd}]/[G_{keto}]$) of the keto carbon of Z-Lys-COCHO was determined to be 1.5 ± 0.1 by quantitative ^{13}C NMR. K_s was assumed to be equal to K_i for Z-Lys-H and $K_{i(obs)}$ was the observed K_i for Z-Lys-COCHO (Table 1). The observed equilibrium constant for hemiketal formation ($K_{HK(obs)}$=[Trypsin-hemiketal]/[Trypsin-glyoxal]) of 682 is similar to values observed with chymotrypsin and subtilisin (Table 2).

3.8. The effective molarity of the catalytic serine hydroxyl group in trypsin

The effective molarity is determined by the ratio $K_{HK(obs)}/K_{H1}$ for the unimolecular process of hemiketal formation within the trypsin-inhibitor complex ($K_{HK(obs)}$) and the second order process by which water reacts with the glyoxal inhibitor to form the hydrated glyoxal (K_{H1}). The effective molarity of the active site serine hydroxyl group of trypsin is 25,300 M showing that it is 25,300 times more reactive than the hydroxyl groups of water. This gives a stabilisation of −25.1 kJ/mol (Table 2).

3.9. Effect of pH on binding and hemiketal formation between trypsin and Z-Lys-COCHO

From pH 7.2 to pH 5.0 there is 20 fold increase in K_i for Z-Lys-COCHO but only a 5 fold increase in K_i for Z-Lys-H (Table 3). A decrease in binding at low pH is expected for both inhibitors due to the protonation of the carboxylate side chain of aspartate-189 in the S_1 specificity pocket of trypsin preventing its ion pair interaction with the positively charged lysine side chain of Z-Lys-H or Z-Lys-COCHO. From pH 7.2 to pH 10.3 K_i for Z-Lys-H decreased slightly while the K_i for Z-Lys-COCHO is doubled (Table 3).

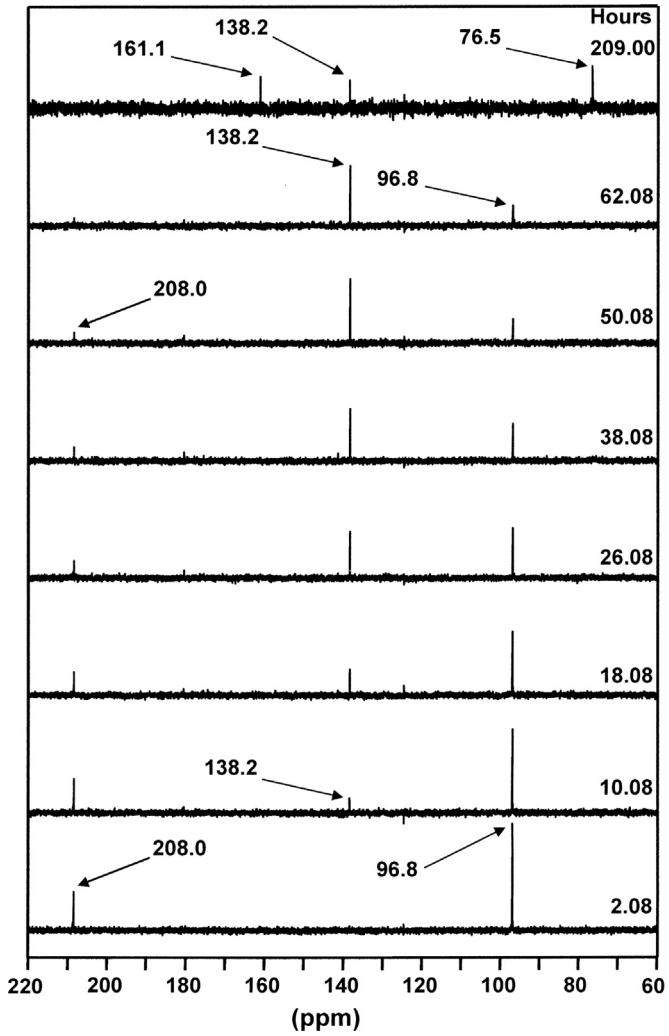

Fig. 4. ^{13}C NMR of Schiff base formation by Z-Lys-^{13}COCHO at pH 7.0. The conditions used for proton decoupling are described in the Materials and methods section, NMR parameters were: 32768 time domain points; spectral width 236.6 ppm; acquisition time 0.55 s; 9.1 s relaxation delay time; 90° pulse angle; exponential weighting factor of 2 Hz; number of transients recorded per spectrum were 1480 except for the spectrum recorded after 209 h which had 760 transients recorded. Sample conditions were: 3 ml of 1.1 mM Z-Lys-^{13}COCHO, 20 mM potassium phosphate buffer, pH 7.0.

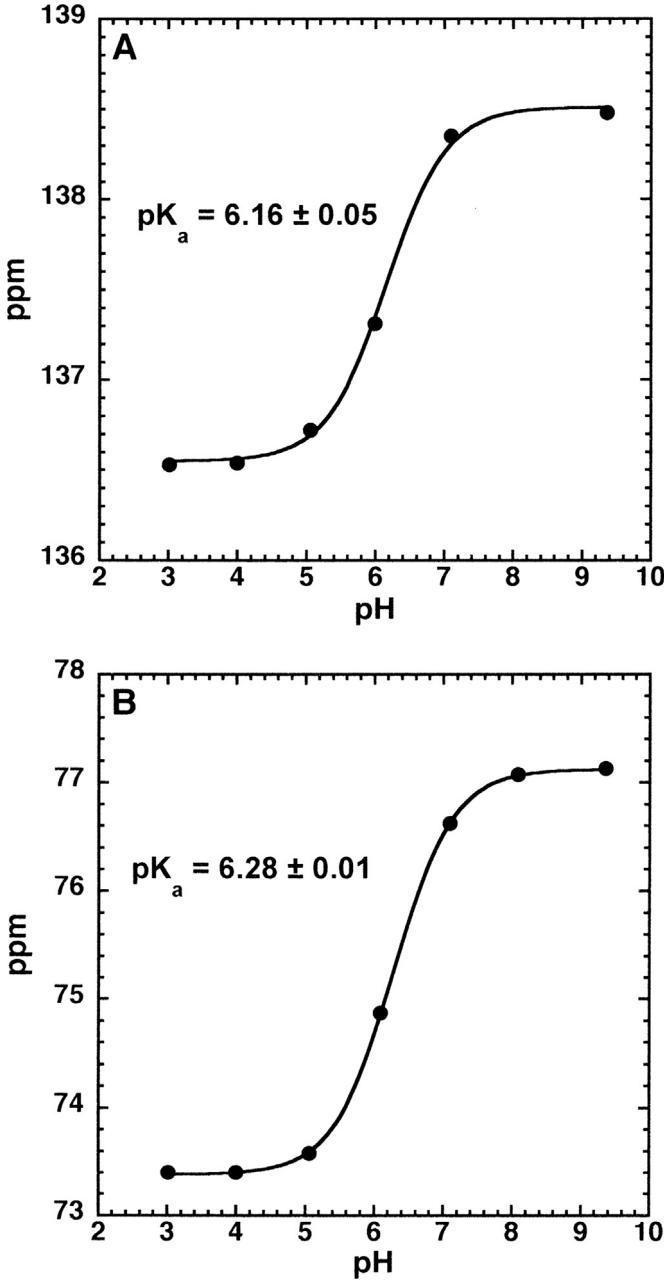

Fig. 5. Effect of pH on the chemical shifts of the ^{13}C NMR signals from the Schiff bases formed from Z-Lys-^{13}COCHO. In (A) and (B) the continuous line was calculated using the equation $\delta_{obs}=\delta_1/(1+K_a/[H])+\delta_2/(1+[H]/K_a)$ and the fitted parameters: (A) pKa = 6.16 ± 0.05, δ_1 = 136.55 ± 0.01 ppm and δ_2 = 138.51 ± 0.02 ppm; (B) pKa = 6.28 ± 0.01, δ_1 = 73.38 ± 0.01 ppm and δ_2 = 77.12 ± 0.01 ppm.

Hemiketal formation was optimal at pH 7.2 but decreased 4–2.5 fold at pHs 5.0 and 10.3 (Table 3).

3.10. ^{13}C NMR spectra of trypsin inhibited by Z-Lys-CO^{13}CHO

In aqueous solutions Z-Lys-CO^{13}CHO had NMR signals (Fig. 7a) at 90.4 ppm due to the hydrated glyoxal aldehyde carbon when the glyoxal keto-carbon is hydrated (Structure 1 in Scheme 2) and 88.7 ppm due to the hydrated aldehyde carbon when the glyoxal keto carbon is not hydrated (Structure 2 in Scheme 2). The small signal at 94.2 ppm is due to a small amount of polymerized inhibitor (Structure 3 in Scheme 3) in the inhibitor sample (Fig. 7a) which is not affected by the addition of trypsin (Fig. 7a–e). On adding the inhibitor (Fig. 7a) to trypsin (Fig. 7b) at pH 4.8 no new signals were detected at pH 4.8 (Fig. 7c). On increasing the pH to 5.6 a new signal at 205.3 ppm was produced and the signals at 90.4 ppm and 88.7 ppm due the free inhibitor decreased (Fig. 7d). At pH 6.3, 6.8 and 7.2 the signals at 90.4 ppm and 88.7 ppm were no longer observed (Fig. 7e–g). However, on reducing the pH to 3.2 the signal at 205.3 ppm was lost and the signals at 90.4 ppm and 88.7 ppm due to the free inhibitor were restored (Fig. 7h) showing that these changes are reversible. Based on its K_i value (Table 3), the inhibitor is optimally bound (97%) at neutral pHs and the signal at 205.3 had its optimal intensity at pH 6.8 (Fig. 7f) showing that this signal is due to an enzyme bound species. A methine carbon (CH) is expected to have a linewidth of 25–50 Hz when rigidly attached to a protein like trypsin with an Mr value of 24,000 [35,36] Therefore the linewidth of 45 ± 2 Hz for the signal at 205.5 ppm is consistent with the inhibitor being bound rigidly to trypsin. A similar signal at 205.5 ppm has been observed with Z-Ala-Pro-Phe-CO^{13}CHO bound to chymotrypsin and this was assigned to the non-hydrated glyoxal aldehyde carbon rigidly attached to chymotrypsin [15,17]. We assign the signal at

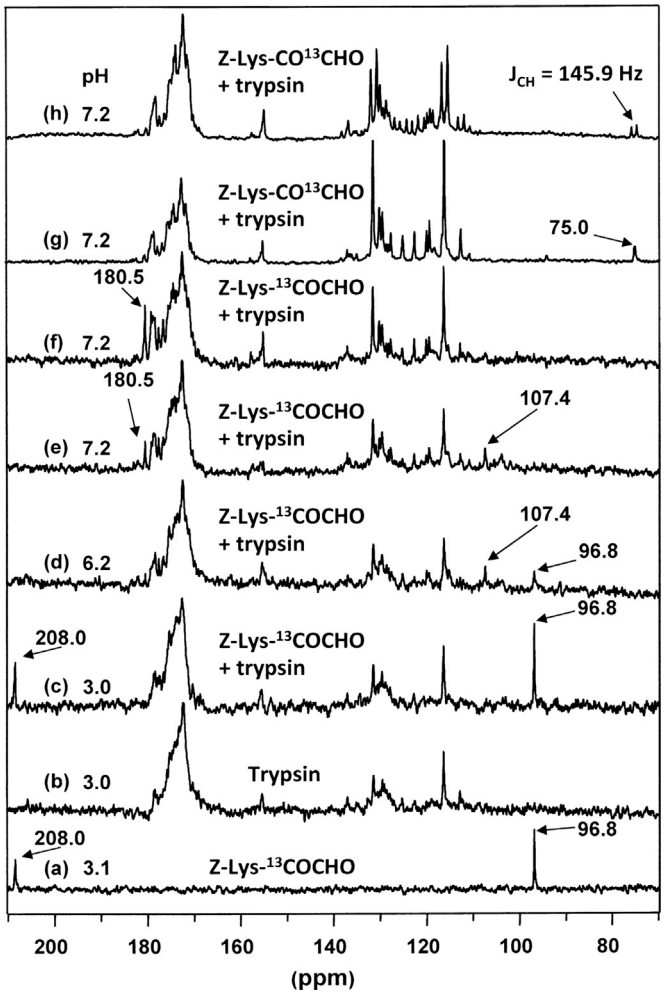

Fig. 6. Effect of pH on the ^{13}C NMR signals from the ^{13}C-enriched carbon of Z-Lys-^{13}COCHO in the presence of trypsin. Spectra (c,d,e) were obtained when Z-Lys-^{13}COCHO (Spectrum (a)) was added to trypsin (Spectrum (b)) at pHs 3.0, 6.2 and 7.2 respectively. Spectrum (f) was obtained after incubating Z-Lys-^{13}COCHO with trypsin for 26 h at pH 7.2. Spectrum (g) was obtained after incubating Z-Lys-CO^{13}CHO with trypsin for 30 h at pH 7.2. Spectrum (h) is a proton coupled spectrum of the sample used for spectrum (g). The conditions used for proton decoupling are described in the Materials and methods section, For spectra (a)–(f) NMR parameters were: 32768 time domain points; spectral width 236.5 ppm; acquisition time 0.55 s; 8 s relaxation delay time; 90° pulse angle; exponential weighting factor of 20 Hz. For spectra (g)–(h) NMR parameters were: 16384 time domain points; spectral width 219.2 ppm; acquisition time 0.15 s; 0.6 s relaxation delay time; 90° pulse angle; exponential weighting factor of 20 Hz. Spectrum (h) was not proton decoupled. The number of transients recorded per spectrum were (a) 1638, (b)–(d) 256, (e)–(f) 1680, (g) 17,792, (h) 71,168. Sample conditions were 3 ml: (a) 0.56 mM Z-Lys-^{13}COCHO, ~1 mM HCl, pH 3.1; (b)1.78 mM fully active trypsin, 21 mM $CaCl_2$; (c) 1.72 mM fully active trypsin, 1.87 mM Z-lys-^{13}COCHO; (d) 1.64 mM fully active trypsin, 1.87 mM Z-lys-^{13}COCHO; (e) 0.87 mM fully active trypsin, 0.93 mM Z-lys-^{13}COCHO; (f) 0.87 mM fully active trypsin, 0.87 mM Z-lys-^{13}COCHO; (g-h) 1.12 mM fully active trypsin, 1.41 mM Z-lys-CO^{13}CHO.

205.3 ppm in the same way to the non-hydrated aldehyde carbon of Z-Lys-CO^{13}CHO rigidly bound to trypsin (Structure 4 in Scheme 2).

3.11. ^{13}C NMR spectra of trypsin inhibited by Z-Lys-^{13}COCHO

In aqueous solutions Z-Lys-^{13}COCHO had NMR signals (Fig. 6a) at 208.0 ppm due to the glyoxal keto carbon (Structure 2 in Scheme 2) and 96.8 ppm due to the hydrated keto carbon (Structure 1 in Scheme 2). On adding Z-Lys-^{13}COCHO (Fig. 6a) to trypsin (Fig. 6b) at pH 3.0 no new signals were observed (Fig. 6c). However, on adding

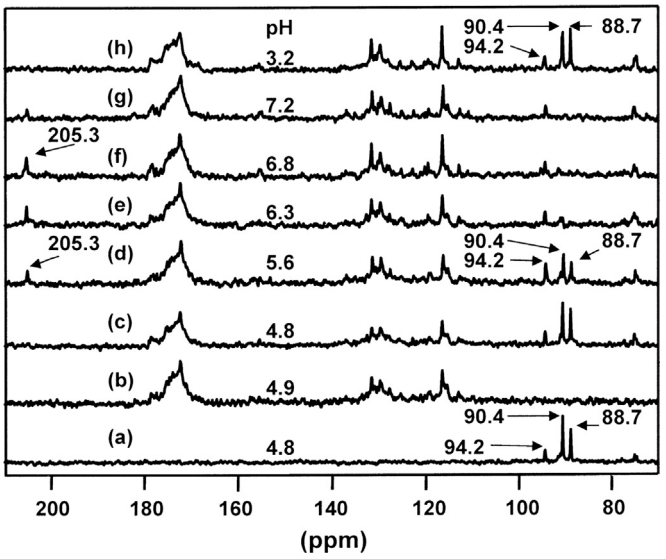

Fig. 7. Effect of pH on the ^{13}C NMR signals from the ^{13}C-enriched carbon of Z-Lys-CO^{13}CHO in the presence of trypsin. The conditions used for proton decoupling are described in the Materials and methods section, For spectra (a)–(h) NMR parameters were; 8192 time domain points; spectral width 219.2 ppm; acquisition time 0.15 s; 0.6 s relaxation delay time; 90° pulse angle; exponential weighting factor of 20 Hz; 2048 number of transients recorded per spectrum. Sample conditions were 3 ml: (a) 1.1 mM Z-Lys-CO^{13}CHO, pH 3.1; (b) 1.13 mM fully active trypsin, 20 mM $CaCl_2$; (c) 1.12 mM fully active trypsin, 1.40 mM Z-lys-CO^{13}CHO, 20 mM $CaCl_2$; (d) 1.13 mM fully active trypsin,1.40 mM Z-lys-CO^{13}CHO, 20 mM $CaCl_2$; (e) 1.12 mM fully active trypsin, 1.4 mM Z-lys-^{13}COCHO, 20 mM $CaCl_2$; (f) 1.12 mM fully active trypsin, 1.39 mM Z-lys-CO^{13}CHO, 20 mM $CaCl_2$; (g) 1.12 mM fully active trypsin, 1.39 mM Z-lys-CO^{13}CHO, 20 mM $CaCl_2$; (h) 1.11 mM fully active trypsin, 1.38 mM Z-lys-CO^{13}CHO, 20 mM $CaCl_2$.

Z-Lys-^{13}COCHO to trypsin at pH 6.2 the signals at 96.8 ppm and 208.0 ppm due to the free inhibitor decreased in intensity and a new signal was detected at 107.4 ppm (Fig. 6d). A similar signal at ~107 has been observed with chymotrypsin [15,17] and subtilisin [19,20] and is assigned in the same way to structure 4 in Scheme 2. At pH 7.2 the signal at 107.4 decreased in intensity with time (Fig. 6e and f) and a new signal at 180 ppm (Fig. 6e and f) slowly appeared ($t_{1/2}$=2.9 h). In the proton coupled spectrum (not shown) the signal at ~180 ppm was a singlet showing there were no directly bonded protons. This signal titrated from 177.22 ± 0.04 ppm to 180.49 ± 0.03 ppm according to a pKa of 3.19 ± 0.07 (Fig. 8A). The chemical shift value, titration shift and pKa value show that the keto carbon has been converted to a carboxylate group. When a sample of Z-Lys-CO^{13}CHO was incubated with trypsin for a similar time at pH 7.2 the signals at 90.4 and 88.7 ppm were replaced ($t_{1/2}$=2.9 h) by a signal at 75 ppm (Fig. 6g) which gave a doublet (J_{CH} = 145.9 ± 2.4 Hz) when proton coupled (Fig. 6h) showing that it had one directly bonded proton. The carbinolamine species (Structure 5 in Scheme 3) had a similar chemical shift but its coupling constant of ~160 Hz is significantly larger. The signal at ~75 ppm titrated from 73.70 ± 0.02 ppm to 75.36 ± 0.02 ppm according to a pKa of 3.25 ± 0.07 (Fig. 8B).

4. Discussion

It is clear from our results that the inhibitor can undergo an intramolecular cyclisation reaction whereby the ε-amino group of the inhibitor forms a Schiff base with glyoxal aldehyde carbonyl carbon (Structure 1 in Scheme 5). The keto carbon of the cyclised inhibitor undergoes a rapid enolisation reaction to form an enol (Structures 2 and 3 in Scheme 5) which hydrolyses to give an alcohol (Structures 4 and 5 in Scheme 5). In an earlier study[15] with Z-Ala-Pro-Phe-

Table 2
The effective molarity of the catalytic serine of the serine proteases trypsin, chymotrypsin and subtilisin when forming hemiketals with glyoxal inhibitors.

Enzyme	pH	$K_{i(obs)}$[a] (μM)		$K_{HK(obs)}$	K_{H1} (M^{-1})	Effective Molarity (M)	ΔG at 25 °C (kJ mol^{-1})
		ZK-H	ZK-COCHO				
Trypsin	7.2	2240 ± 290	8.20 ± 0.53	682	0.0270	25,300	−25.1
		ZAAF-H	ZAAF-COCHO				
α-Chymotrypsin	7.2	166 ± 9	0.365[b]	1170	0.0284	41,200	−26.3
Subtilisin Carlsberg	7.1	97.6 ± 12.6	0.0876 ± 0.016	2870	0.0284	101,000	−28.6
		ZAPF-H	ZAPF-COCHO				
α-Chymotrypsin	7.2	77.4 ± 6.4	0.0335[b]	5270	0.023	229,000	−30.6
Subtilisin Carlsberg	7.2	1600 ± 600	1.00 ± 0.03	3650	0.023	159,000	−29.7

[a] Errors are the standard deviations of 3 determinations.
[b] [17].

Table 3
Effect of pH on hemiketal formation in glyoxal inhibitor complexes with trypsin.

pH	$K_{i(obs)}$ (μM)[a]		$K_{HK(obs)}$
	Z-Lys-H	Z-Lys-COCHO	
5.0	11200 ± 100	165 ± 16	169
7.2	2240 ± 290	8.2 ± 0.5	682
10.3	1870 ± 150	17.0 ± 0.1	274

[a] Errors are the standard deviations of 3 determinations.

COCHO it was shown that at alkaline pHs the glyoxal inhibitor undergoes an internal Cannizzaro reaction [37] forming an α-hydroxycarboxylic acid (Z-Ala-Pro-Phe-CH(OH)COOH). It was also shown [15] that both a C1-C2 hydride shift and a C2-C1 alkyl shift occurred with glyoxal inhibitors. Therefore when the glyoxal aldehyde carbon ($RCO^{13}CHO$) was ^{13}C-enriched the Cannizzaro reactions resulted in half the α-hydroxycarboxylic acid being ^{13}C-enriched in the carboxylate carbon($RCH(OH)^{13}COOH$) due to a C2-C1 alkyl shift and the other half being enriched in the hydroxy-carbon($R^{13}CH(OH)COOH$) due to a C1-C2 hydride shift. These products were also formed if the glyoxal keto carbon($RCO^{13}CHO$) was ^{13}C-enriched. Neither of these reaction products were observed when Z-Lys-^{13}COCHO or Z-Lys-$CO^{13}CHO$ were incubated at alkaline pH instead there was intramolecular Schiff base formation. This shows that the intramolecular cyclisation via Schiff base formation is a much faster reaction than the Cannizzaro reaction in the free Z-Lys-COCHO inhibitor.

In contrast, at pH ~7 in the presence of trypsin, intramolecular cyclisation of Z-Lys-COCHO to form a Schiff base was not detected. Under the experimental conditions given in Fig. 6e and f ~94% of the inhibitor was bound to trypsin. Therefore we conclude that the binding of the ε-amino group of the inhibitor in the S_1 specificity site of trypsin inhibits its intramolecular reaction with the glyoxal aldehyde carbon to form a Schiff base. Instead, with Z-Lys-$CO^{13}CHO$ and Z-Lys-^{13}COCHO new signals at 205.3 ppm (Fig. 7d–g) and 107.4 ppm (Fig. 6d and e) were detected respectively on adding trypsin. Similar signals have been observed with glyoxal inhibitors with both chymotrypsin [15,17] and subtilisin [19,20]. These signals have been assigned [15,17,19,20] to a hemiketal (Structure 4 in Scheme 2) formed by the reaction of the active site serine hydroxyl group with the glyoxal keto carbon (Scheme 2). However, with Z-Lys-^{13}COCHO at pH~7, there was also the slow formation ($t_{1/2}$= 2.9 h) of signal at ~180 ppm which had no directly bonded protons and titrated from 177.22 ± 0.04 to 180.49 ± 0.03 with a pKa of 3.19 ± 0.07 (Fig. 8A). With Z-Lys-$CO^{13}CHO$ and trypsin at pH~7 there was also the slow formation ($t_{1/2}$ 2.9 h) of a signal at ~75 ppm which had one directly bonded proton (J_{CH}=145.9 ± 2.4 Hz) and titrated from 73 to 75 ppm with a pKa of 3.25 (Fig. 8B). The chemical shift values, proton couplings, titration shifts and pKa values confirm that a hydroxycarboxylic acid (Structures 3 and 4 in Scheme 6) has been formed[15] from the hemiketal species (Structure 1 in Scheme 6). As both Z-Lys^{13}COCHO and Z-Lys-$CO^{13}CHO$ only produced one ^{13}C-enriched hydroxycarboxylic acid we conclude that when the inhibitor is bound to trypsin as a hemiketal it only undergoes one internal Cannizzaro reaction via a C2 to C1 alkyl shift (Scheme 6). This also occurred when chymotrypsin was incubated with glyoxal inhibitors [15] and it was suggested that as the carbonyl carbon of the glyoxal aldehyde group is expected to be in the same position as the peptide nitrogen atom of the leaving group in a substrate, and so it will also be subjected to general acid catalysis by His-57 promoting its formation. In contrast the C1 to C2 hydride shift will be prevented by formation of the tetrahedral hemiketal. Therefore it appears that the C2 to C1 alkyl shift mechanism predominates when either trypsin or chymotrypsin react with glyoxal inhibitors. However, at pH 7.0 the C2-C1 alkyl shift is ~3 × faster with trypsin ($t_{1/2}$=2.9 h) than chymotrypsin [15].

The binding of Z-Arg-COOH to trypsin was only ~2 fold tighter than the binding of Z-Lys-COOH (Table 1). In contrast the inhibition by methyl or ethyl guanidines is 20–30 times more effective than inhibition by the corresponding amines [38]. Likewise k_{cat}/K_M for the trypsin catalysed hydrolysis of Bz-Phe-Val-Arg-pna is ~20 times greater than that observed when the arginine residue is replaced by a lysine residue [39]. The fact that the binding of Z-Arg-COOH is not ~20 tighter than Z-Lys-COOH ensures that the better binding and catalytic efficiency of arginine substrates is not

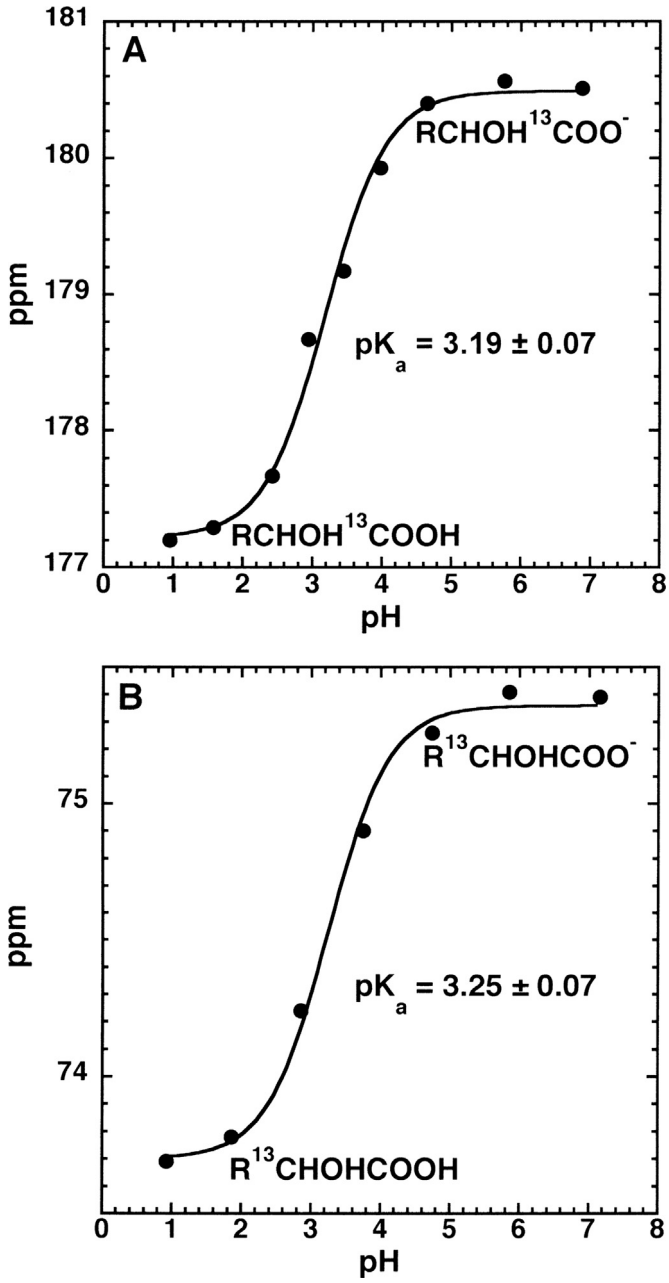

Fig. 8. Effect of pH on the chemical shifts of the ^{13}C NMR signals from the α-hydroxycarboxylic acids formed from Z-Lys-^{13}COCHO and Z-Lys-CO^{13}CHO. In (A) and (B) the continuous line was calculated using the equation $\delta_{obs}=\delta_1/(1+K_a/[H])+\delta_2/(1+[H]/K_a)$ and the fitted parameters: (A) pKa = 3.19 ± 0.07, δ_1 = 177.22 ± 0.04 ppm and δ_2 = 180.49 ± 0.03 ppm; (B) pKa = 3.25 ± 0.07, δ_1 = 73.70 ± 0.02 ppm and δ_2 = 75.36 ± 0.02 ppm.

cancelled out by more effective product inhibition by Z-Arg-COOH compared to Z-Lys-COOH. Therefore arginine substrates are more effective substrates than their lysine analogues.

The values of K_{HKobs} (K_{HKobs} = [Hemiketal]/[> C = O]) in Tables 2 and 3 can be used to estimate the amount of hemiketal stabilization. Hemiketal stabilization by trypsin with Z-Lys-glyoxal is similar to that observed with chymotrypsin and Z-Ala-Ala-Phe-COCHO even though binding of the inhibitor is at least 10 × more effective with chymotrypsin (Table 2). Likewise for Z-Ala-Pro-Phe-COCHO, hemiketal stabilization by with subtilisin and chymotrypsin is similar even though binding differs by a factor of 20–30 (Table 2). This shows that better binding by the peptide portion of a glyoxal inhibitor does not lead a corresponding increase in the amount of hemiketal formed. For trypsin hemiketal formation is maximal at pH 7.2 but decreases at pHs 5.0 and 10.3 (Table 3). A similar result was obtained with chymotrypsin where the decrease in K_{HKobs} at low pH was attributed to protonation of the hemiketal oxyanion and the decrease at high pH was attributed to a known conformational change in chymotrypsin at high pH [24]. No such conformational change is known to occur in trypsin and so we cannot explain the decrease in K_{HKobs} at pH 10.3 (Table 3).

The large effective molarities observed with trypsin, chymotrypsin and subtilisin (Table 2) clearly demonstrate that the reactivity of the catalytic serine hydroxyl group in the serine proteases is greatly enhanced relative to the reactivity of the hydroxyl groups of water.

5. Conclusions

The aldehyde group of the free glyoxal inhibitor Z-Lys-COCHO cyclizes by initially forming a Schiff base with the ε-amino group

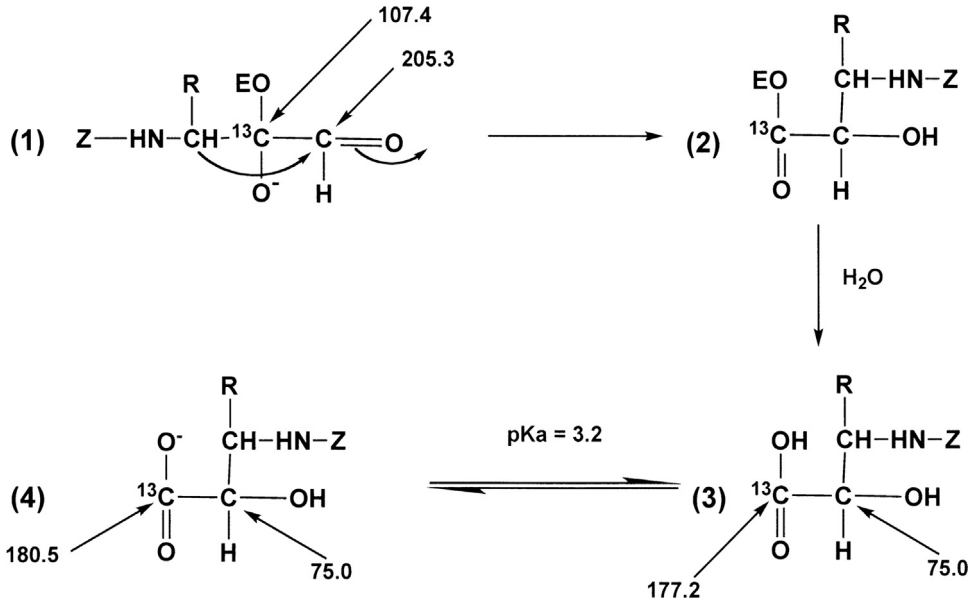

Scheme 6. Trypsin catalysed breakdown of Z-Lys-COCHO. R=–$(CH_2)_4$–NH_3^+, EO represents the oxygen atom of the catalytic serine hydroxyl group of trypsin.

of the inhibitor. This cyclisation reaction is inhibited by the binding of the ε-amino group of the inhibitor in the S_1 specificity pocket of trypsin. Glyoxal inhibitors bound to trypsin and chymotrypsin undergo an internal Cannizaro reaction via a C2 to C1 alkyl shift producing a hydroxycarboxylic acid.

Trypsin like chymotrypsin and subtilisin forms a hemiketal with the keto-carbon of a specific glyoxal inhibitor analogous to the tetrahedral intermediate formed during catalysis. Hemiketal stabilization by trypsin is similar that observed with chymotrypsin. Better binding by the peptide portion of specific glyoxal inhibitors does not make a corresponding increase in the amount of hemiketal formed with the serine proteases. The catalytic serine hydroxyl group of trypsin is ~25,000 times more reactive than the hydroxyl groups of water.

Acknowledgements

This work was supported by University College Dublin and the Irish Research Council Government of Ireland Postgraduate Scholarship Scheme Grant no. 355593.

Appendix A. Supplementary material

Supplementary data associated with this article can be found in the online version at http://dx.doi.org/10.1016/j.bbrep.2015.12.015.

References

[1] L. Hedstrom, Serine protease mechanism and specificity, Chem. Rev. 102 (2002) 4501–4523.
[2] J. Kraut, Serine proteases: structure and mechanism of catalysis, Ann. Rev. Biochem. 46 (1977) 331–358.
[3] J. Fastrez, A.R. Fersht, Mechanism of chymotrypsin-structure, reactivity, and nonproductive binding relationships, Biochemistry 12 (1973) 1067–1074.
[4] R. Wolfenden, Transition state analog inhibitors and enzyme catalysis, Annu. Rev. Biophys. Bioeng. 5 (1976) 271–306.
[5] T.P. O'Connell, R.M. Day, E.V. Torchilin, W.W. Bachovchin, J.P.G. Malthouse, A ^{13}C-NMR study of the role of Asn-155 in stabilizing the oxyanion of a subtilisin tetrahedral adduct, Biochem. J. 326 (1997) 861–866.
[6] T.P. O'Connell, J.P.G. Malthouse, A study of the stabilization of the oxyanion of tetrahedral adducts by trypsin, chymotrypsin and subtilisin, Biochem. J. 307 (1995) 353–359.
[7] T.P. O'Connell, J.P.G. Malthouse, Determination of the ionization state of the active-site histidine in a subtilisin-(chloromethane inhibitor) derivative by ^{13}C-NMR, Biochem. J. 317 (1996) 35–40.
[8] D.B. O'Sullivan, T.P. O'Connell, M.M. Mahon, A. Koenig, J.J. Milne, T. P. Fitzpatrick, J.P.G. Malthouse, ^{13}C-NMR study of how the oxyanion pKa values of subtilisin and chymotrypsin tetrahedral adducts are affected by different amino acid residues binding in enzymes subsites S_1-S_4, Biochemistry 38 (1999) 6187–6194.
[9] M.D. Finucane, E.A. Hudson, J.P.G. Malthouse, A ^{13}C-n.m.r. investigation of the ionizations within an inhibitor-alpha-chymotrypsin complex: evidence that both alpha-chymotrypsin and trypsin stabilize a hemiketal oxyanion by similar mechanisms, Biochem. J. 258 (1989) 853–859.
[10] M.D. Finucane, J.P.G. Malthouse, A study of the stabilization of tetrahedral adducts by trypsin and delta-chymotrypsin, Biochem. J. 286 (1992) 889–900.
[11] J.P.G. Malthouse, N.E. Mackenzie, A.S.F. Boyd, A.I. Scott, Detection of a tetrahedral adduct in a trypsin-chloromethyl ketone specific inhibitor complex by ^{13}C NMR, J. Am. Chem. Soc. 105 (1983) 1685–1686.
[12] J.P.G. Malthouse, W.U. Primrose, N.E. Mackenzie, A.I. Scott, ^{13}C NMR Study of the Ionizations within a trypsin-chloromethyl ketone inhibitor complex, Biochemistry 24 (1985) 3478–3487.
[13] W.U. Primrose, A.I. Scott, N.E. Mackenzie, J.P.G. Malthouse, A 13C-n.m.r. investigation of ionizations within a trypsin-inhibitor complex. Evidence that the pKa of histidine-57 is raised by interaction with the hemiketal oxyanion, Biochem. J. 231 (1985) 677–682.
[14] A. MacSweeney, G. Birrane, M.A. Walsh, T.P. O'Connell, J.P.G. Malthouse, T. M. Higgins, Crystal structure of D-chymotrypsin bound to a peptidyl chloromethyl ketone inhibitor, Acta Cryst. D56 (2000) 280–286.
[15] A. Djurdjevic-Pahl, C. Hewage, J.P.G. Malthouse, A ^{13}C-NMR study of the inhibition of delta-chymotrypsin by a tripeptide-glyoxal inhibitor, Biochem. J. 362 (2002) 339–347.
[16] E.A. Murphy, T.P. O'Connell, J.P.G. Malthouse, The synthesis and characterisation of a glyoxal inhibitor of chymotrypsin, Biochem. Soc. Trans. 24 (1996) 129S.
[17] E. Spink, S. Cosgrove, L. Rogers, C. Hewage, J.P.G. Malthouse, ^{13}C and ^{1}H NMR studies of ionizations and hydrogen bonding in chymotrypsin-glyoxal inhibitor complexes, J. Biol. Chem. 282 (2007) 7852–7861.
[18] B. Walker, N. McCarthy, A. Healy, T. Ye, M.A. McKervey, Peptide glyoxals: a novel class of inhibitor for serine and cysteine proteinases, Biochem. J. 293 (1993) 321–323.
[19] A. Djurdjevic-Pahl, C. Hewage, J.P.G. Malthouse, Ionisations within a subtilisin-glyoxal inhibitor complex, Biochim. Biophys. Acta 2005 (1749) 33–41.
[20] N. Howe, L. Rogers, C. Hewage, J.P.G. Malthouse, Oxyanion and tetrahedral intermediate stabilization by subtilisin: detection of a new tetrahedral adduct, Biochim. Biophys. Acta 1794 (2009) 1251–1258.
[21] E. Spink, C. Hewage, J.P.G. Malthouse, Determination of the structure of tetrahedral transition state analogues bound at the active site of chymotrypsin using ^{18}O and ^{2}H isotope shifts in the ^{13}C NMR spectra of glyoxal inhibitors, Biochemistry 46 (2007) 12868–12874.
[22] J.A. Cleary, W. Doherty, P. Evans, J.P. Malthouse, Hemiacetal stabilization in a chymotrypsin inhibitor complex and the reactivity of the hydroxyl group of

the catalytic serine residue of chymotrypsin, Biochim. Biophys. Acta 1844 (2014) 1119–1127.
[23] J.A. Cleary, W. Doherty, P. Evans, J.P. Malthouse, Quantifying tetrahedral adduct formation and stabilization in the cysteine and the serine proteases, Biochim. Biophys. Acta 2015 (1854) 1382–1391.
[24] T. Petrillo, C.A. O'Donohoe, N. Howe, J.P.G. Malthouse, Importance of tetrahedral intermediate formation in the catalytic mechanism of the serine proteases chymotrypsin and subtilisin, Biochemistry 51 (2012) 6164–6170.
[25] S. Cosgrove, L. Rogers, C. Hewage, J.P.G. Malthouse, An NMR study of the inhibition of pepsin by glyoxal inhibitors: mechanism of tetrahedral intermediate stabilization by the aspartyl proteinases, Biochemistry 46 (2007) 11205–11215.
[26] N. Howe, M. Ceruso, E. Spink, J.P. Malthouse, pH stability of the stromelysin-1 catalytic domain and its mechanism of interaction with a glyoxal inhibitor, Biochim. Biophys. Acta 2011 (1814) 1394–1403.
[27] S. Wiejak, E. Masiukiewicz, B. Rzeszotarska, A. Large, Scale synthesis of mono- and di-urethane derivatives of lysine, Chem. Pharm. Bull. 47 (1999) 1489–1490.
[28] T. Chase Jr., E. Shaw, p-Nitrophenyl-p′-guanidinobenzoate HCl: a new active site titrant for trypsin, Biochem. Biophys. Res. Commun. 29 (1967) 508–514.
[29] C. Ortiz, C. Tellier, H. Williams, N.J. Stolowich, A.I. Scott, Diastereotopic covalent binding of the natural inhibitor leupeptin to trypsin: detection of two interconverting hemiacetals by solution and solid-state NMR spectroscopy, Biochemistry 30 (1991) 10026–10034.
[30] R.R. Fraser, J. Banville, F. Akiyama, N. Chuaquioffermanns, C-13 shieldings in syn and anti aldimines and ketimines, Can. J. Chem. 59 (1981) 705–709.
[31] G.A. Olah, D.J. Donovan, Carcinogen chemistry. 2. C-13 nuclear magnetic-resonance spectroscopic study of ambident carbocationic nature of iminium ions and its relevance to aminoalkylating ability of related chemical carcinogens, J. Org. Chem. 43 (1978) 860–865.
[32] H.-O. Kalinowski, S. Berger, S. Braun, Carbon-13 NMR Spectroscopy, Antony Rowe Limited, UK, 1988.
[33] M.I. Page, The mechanism of chemical catalysis used by enzymes. in: The Chemistry of Enzyme Action, vol. 6, Elsevier Science, Amsterdam, Netherlands, 1984, pp. 240–242.
[34] B. Capon, A.K. Sidddhanta, Simple enols. 3. Stereochemistry of simple enols in solution, J. Org. Chem. 49 (1984) 255–257.
[35] J.P.G. Malthouse, ^{13}C NMR of enzymes, Prog. Nucl. Magn. Reson. Spectrosc. 18 (1986) 1–60.
[36] J.P.G. Malthouse, M.D. Finucane, A study of the relaxation parameters of a 13C-enriched methylene carbon and a 13C-enriched perdeuteromethylene carbon attached to chymotrypsin, Biochem. J. 280 (1991) 649–657.
[37] O.H. Wheeler, Reduction of carbonyl groups, in: S. Patai (Ed.), The Chemistry of the Carbonyl Group 1966 Interscience, London, Sydney, New York, pp. 507–566.
[38] T. Inagami, S.S. York, Effect of alkylguanidines and alkylamines on trypsin catalysis, Biochemistry 7 (1968) 4045–4052.
[39] M. Pozsgay, G. Szabo, S. Bajusz, R. Simonsson, R. Gaspar, P. Elodi, Investigation of the substrate-binding site of trypsin by the aid of tripeptidyl-p-nitroanilide substrates, Eur. J. Biochem. 115 (1981) 497–502.